Bone 125 (2019) 74–86

Contents lists available at ScienceDirect

Bone

journal homepage: www.elsevier.com/locate/bone

Full Length Article

HOXA cluster gene expression during osteoblast differentiation involves epigenetic control

Rodrigo A. da Silva[a,b], Gwenny M. Fuhler[b], Vincent T. Janmaat[b], Célio Júnior da C. Fernandes[a], Geórgia da Silva Feltran[a], Flávia Amadeu Oliveira[c], Adriana Arruda Matos[c], Rodrigo Cardoso Oliveira[c], Marcel Rodrigues Ferreira[a], Willian F. Zambuzzi[a,*,1], Maikel P. Peppelenbosch[b,**,1]

[a] Laboratory of Bioassays and Cellular Dynamics, Department of Chemistry and Biochemistry, Institute of Biosciences, São Paulo State University - UNESP, Botucatu, São Paulo 18618-970, Brazil
[b] Department of Gastroenterology and Hepatology, Erasmus MC, University Medical Center Rotterdam, the Netherlands
[c] Department of Biological Sciences, Bauru School of Dentistry, University of São Paulo, Al. Octávio Pinheiro Brisolla, 9-75, 17012-901 Bauru, São Paulo, Brazil

ARTICLE INFO

Keywords:
Bone
Osteoblast
Hox genes
HoxA genes
Differentiation
Development

ABSTRACT

The *HOXA* gene cluster is generally recognized as a pivotal mediator of positional identity in the skeletal system, expression of different orthologues conferring alternative locational phenotype of the vertebrate bone. Strikingly, however, the molecular mechanisms that regulate orthologue-specific expression of different *HOXA* cluster members in gestating osteoblasts remain largely obscure, but in analogy to the processes observed in acute lymphatic leukemia it is assumed that alternative methylation of *HOXA* promoter regions drives position specific expression patterns. In an effort to understand *HOXA* cluster gene expression in osteogenesis we characterize both expression and the epigenetic landscape of the *HOXA* gene cluster during *in vitro* osteoblast formation from mesenchymal precursors. We observe that osteoblast formation *per se* provokes strong upregulation of *HOXA* gene cluster expression, in particular of midcluster genes, and paradoxal downregulation of *HOXA7* and *HOXA10*. These differences in expression appear related to promoter methylation. LnRNAs HOTAIR and HOTTIP, known to modulate *HOXA* expression, are also regulated by their promoter methylation processing, but do not correlate with HOXA cluster expression profile. We thus conclude that *HOXA* expression is profoundly regulated during osteoblast differentiation through canonical methylation-dependent mechanisms but not through the flanking lnRNAs.

1. Introduction

Skeletal phenotype in the body is highly position dependent and bone phenotype is markedly different depending on its exact location in the body. The mechanisms maintaining locational phenotype are highly robust as positional information is faithfully recapitulated even in healing bone [1]. The molecular determinants of positional identity in regenerating bone remain subject to substantial debate but a cardinal role of Homeobox (*HOX*) genes, which provide spatial information affecting both bone position and whole-body morphology in vertebrates, in determining positional identity in this respect has remained unchallenged. HOX genes constitute a family of evolutionarily-conserved transcription factors that regulate patterning of the developing skeleton [2]. Thus, understanding the mechanisms that control their expression is of evident importance for understanding bone physiology.

HOX genes are organized in four distinct gene clusters [3,4], denominated as the *HOXA* cluster through the *HOXD* cluster and each maps to a different chromosome. In turn, each *HOX* cluster has nine to eleven protein-coding transcription units, which within a cluster are transcribed from the same strand of DNA, and in conjunction give rise to thirteen paralogous genes [5–7]. Characteristically, *HOX* gene expression occurs in a temporal and spatial order that corresponds to their chromosomal order within the cluster, called collinearity [8,9]. The *HOX* genes that map to the 3′ end of the clusters are transcribed earlier

* Correspondence to: W.F. Zambuzzi, UNESP - Campus de Botucatu - Instituto de Biociências, Rua Profª. Drª. Irina Delanova Gemtchujnicov, s/n°, 18618-693 Botucatu, SP, Brazil.
** Correspondence to: M.P. Peppelenbosch, Na-1007; Erasmus MC, PO Box 2040, NL-3000 CA Rotterdam, the Netherlands.
E-mail addresses: w.zambuzzi@unesp.br (W.F. Zambuzzi), m.peppelenbosch@erasmusmc.nl (M.P. Peppelenbosch).
[1] These authors share senior authorship.

https://doi.org/10.1016/j.bone.2019.04.026
Received 19 March 2019; Received in revised form 25 April 2019; Accepted 30 April 2019
Available online 01 May 2019

during development and more anteriorly along the main body axis [10,11], whereas those found at 5′ of the cluster are transcribed and at more posterior locations [12]. Various mechanism controlling *HOX* gene expression have been postulated including higher order chromatin organization, regulation through morphogenetic gradients and through the various species of non-coding RNAs transcribed from the *HOX* clusters [13–15]. The importance of these various mechanisms for governing expression of specific *HOX* gene orthologues in osteoblastogenesis remains, however, obscure at best.

In the context of osteoblastogenesis, the *HOXA* cluster excites special interest. All proteins encoded by *HOXA* cluster genes have important roles in proper skeletal development. *Hoxa1* and *Hoxa2* mutants possess many defects in skeletal elements of the skull [16–18]. *Hoxa2* also regulates osteogenic differentiation by inhibiting bone morphogenetic protein signaling [19]. *Hoxa3*$^{-/-}$ mice have a variety of skeletal defects which include improper positioning of the neck bones and positioning of the clavicle to the axis rather than at the level of the two cervical vertebrae caudal to the axis [20,21]. Animals genetically deficient in *Hoxa4* develop ribs on the seventh cervical vertebra [22]. Analysis of the skeleton of mice having a specific *Hoxa5* deletion shows that these animals display a number of homeotic transformations, restricted to the cervical and thoracic regions, which include the posterior transformation of the seventh cervical vertebra to a thoracic vertebra with associated ribs. Prenatal exposure to boric acid causes alterations of the axial skeleton in rat embryos that are accompanied by a cranial shift of the anterior limit of expression of *Hoxa6* [23]. Overexpression of *Hoxa7* (also known as *Hox11*) provokes perinatal mortality of transgenic animals and is accompanied by multiple craniofacial anomalies, such as cleft palate, open eyes at birth, and nonfused pinnae [24]. Although Hoxa9$^{-/-}$ animals appear externally normal, the animals display vertebral anteriorisations in the lumbar region including supernumerary ribs [25]. *HOXA10* can directly activate osteogenesis through *RUNX2*-dependent and *RUNX2*-independent pathways although its deletion [26], while causing homeotic transformation in the vertebrae, is not associated with problems with osteogenesis *per se.* Also Hand–Foot–Genital syndrome (OMIM #140000), an infrequent autosomal dominant disease developing as the result of loss-of-function of HOXA13 is characterized by skeletal anomalies [27]. Thus, the evidence that the *HOXA* cluster determines positional identity of the bone and drives its development is compelling. Nevertheless, the mechanisms contributing to proper expression of different *HOXA* paralogues remain largely uncharacterized. Current thinking on the mechanisms that govern expression of *HOXA* cluster genes in osteogenesis is to an important extent driven by analogy to the information available in leukemic disease. In acute myeloid leukemia and myelodysplastic syndromes, *NUP98* can become fused to several partner genes, including *HOXA9* [28], which in turn regulates its expression [29]. However, this is unlikely to be a major mechanism controlling *HOXA* gene expression in osteogenesis. Also, in the context of leukemia especially methylation has emerged as an important mechanism controlling expression of *HOXA* cluster members [30]. Inactivation of *HOXA* genes by hypermethylation in myeloid and lymphoid malignancy is frequent and associated with poor prognosis [31]. Whether methylation is important as an expression controlling mechanism for the *HOXA* cluster in osteogenesis has not been explored. Finally, the *HOXA* cluster is characterized by the presence of a flanking long non-coding RNA (lnRNAs) at the 5′ side – HOTTIP, which is required for activation of the five prime HoxA genes [32] through maintaining active chromatin through chromosomal looping in fibroblasts [13]. Whether osteogenesis involves HOTTIP regulation remains unexplored. In addition to HOTTIP, the *HOXA* cluster is also regulated by a lcRNA present in the *HOXC* cluster - HOTAIR. The importance of HOTAIR in osteogenesis is evident, as its knockout provokes lumbosacral bone loss and carpal bone fusion [33] and the lncRNA is downregulated upon osteogenesis [34]. These HOTAIR effects, however, have been linked to *HOXD* cluster regulation and not to expression of *HOXA* cluster members. Thus, despite their obvious relevance for cell fate in the bone, there is paucity of insight as to the mechanisms that govern the expression *HOXA* cluster members during osteogenesis.

The above-mentioned considerations prompted us to investigate *HOXA* regulation during osteogenesis and in order to better address this issue, we employed an *in vitro* model to recapitulate osteoblast differentiation up to 28 days. Physiologically-active osteoblasts were obtained from healthy human donors and the importance of the *HOXA* genes cluster family was evaluated in this phenotype, as well as the influence of the epigenetic landscape on modulating these genes. *In toto*, our results show *HOXA* genes are important drivers of osteogenesis and their expressions are fine-tuned by (de)methylation of specific CpG islands found in their promoter region.

2. Material and methods

2.1. Reagents

L-Ascorbic acid (**A4544**), β-Glycerophosphate (69442), Dexamethasone (D2915) and oligonucleotides for gene expression and promoter methylation were purchased from Sigma Chemical Co. (St. Louis, MO, USA). SYBR Green master mix, TRIzol (15596018), DNase I (18068015), and High-Capacity cDNA Reverse Transcription were bought from Life Technologies/Molecular Probes, Inc. (Eugene, OR, USA). T4-β-glucosyltransferase (T4-BGT) *Msp*I and *Hpa*II restriction enzymes were obtained from New England Biolabs (Beverly, MA, USA). All the other chemicals and reagents used in this study were of analytical grade purchased from commercial sources.

2.2. Cell culture

Primary healthy human osteoblast cells (HOEL) were kindly provided by Dr. José Mauro Granjeiro (Bioengineering Program, National Institute of Metrology, Quality and Technology, Duque de Caxias, Rio de Janeiro, Brazil). HOEL cells were isolated from human bone explants resulting from arthroplasty surgical procedures in otherwise adult healthy donors at the University Hospital Antonio Pedro. Consent was obtained from all subjects by the Fluminense Federal University and carried out in agreement with a local Ethic Committee's register number: #232/08. Cells were cultured in Dulbecco's Modified Eagle's medium low glucose (DMEM; LONZA, Walkersville, MD, USA) supplemented with 10% fetal bovine serum (FBS; Gibco, Grand Island, NY, USA), 100 U/mL of penicillin and 100 μg/mL of streptomycin (Nutricel, Campinas, SP, Brazil) at 37 °C in a humidified atmosphere containing 5% CO_2. Viability and cell density were determined by the trypan blue dye exclusion test.

2.3. In vitro osteoblast-differentiation model

HOEL cells (25×10^4 cells) were seeded into 6-well plates in low glucose DMEM supplemented with 10% FBS and antibiotics. After 24 h of incubation at 37 °C in a humidified atmosphere containing 5% CO_2, the medium was replaced by a conventional osteogenic differentiation medium (basal culture medium DMEM supplemented with ascorbic acid at 50 μg/mL, β-glycerolphosphate 10 mmol L^{-1}, dexamethasone 10 nmol L^{-1}, 10% FBS, and penicillin/streptomycin 1%) for 28 days. The control group was maintained in basal medium DMEM supplemented with 10% FBS and antibiotics.

2.4. Alizarin red, alkaline phosphatase and cell morphology stainings

For alizarin red S, alkaline phosphatase and hematoxylin-eosin stainings, HOEL and MC3T3-E1 cells (4×10^4 cells) were cultured in 24-well plates up to 28 days with osteogenic medium. Thereafter, the cells were fixed in phosphate-buffered 10% formalin, and then washed with Wash Buffer (0.05% Tween in 20 mL in PBS free of Ca^{2+} and

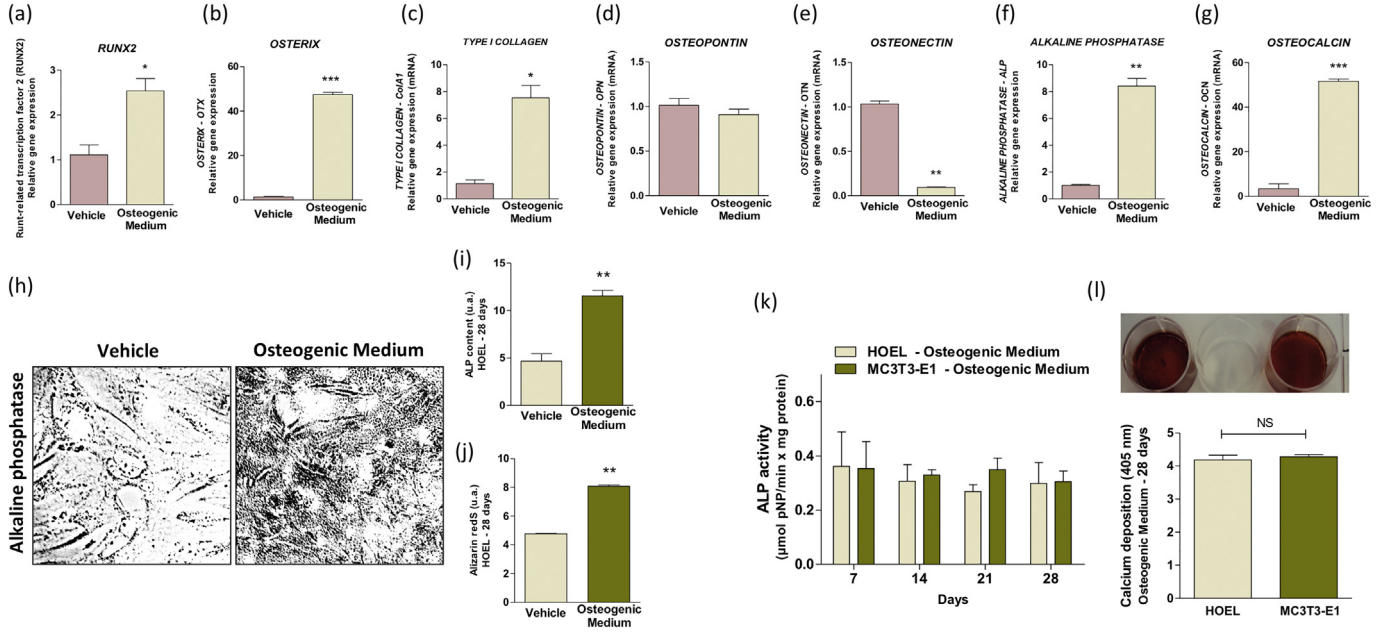

Fig. 1. Osteogenic differentiation of human osteoblasts. Human osteoblasts, isolated from bone explants of human volunteers, were exposed to a convention osteogenic differentiation medium (see Material and methods section). Control cultures and osteogenic cultures were contrasted 28 days later. mRNA levels were analyzed by qPCR. Diagrams show the chances in Runt-related transcription factor 2 (*RUNX2*) (a), transcription factor Sp7 (OSTERIX – *OTX*) (b), Type I collagen (*COL1A1*) (c), Osteopontin (*OPN*) (d), Osteonectin (*OTN*) (e), *Alkaline phosphatase* (*ALP*) (f), *Osteocalcin* (*OCN*) (g). The *in situ* morphological aspect of alkaline phosphatase (h) as well as a quantification of alkaline phosphatase enzymatic activity (i) is also shown, as is a quantification of Alizarin red S levels (j). A comparison to a conventional osteogenic immortalized murine cell models for alkaline phosphatase activity (k) and bone disposition (l) is provided as well. The relative gene expression levels were determined using the cycle threshold (Ct) method and shown in a graphical format with normalized values as a function of the control -assigned value 1. The results are represented as mean ± standard deviation of three independent experiments. *p < 0.05, **p < 0.001 and ***p < 0.0001.

Mg^{2+}). Afterwards, the cells were kept for 10 min in an Alkaline Phosphatase (ALP) solution (SIGMAFAST BCIP/NBT tablet) and 30 min with 2% Alizarin-Red S at room temperature in the dark. For hematoxylin-eosin, the cells were stain for 7 min in hematoxylin and 3 min in eosin in water and dehydrated. Next, the cell was extensively washed with PBS to eliminate nonspecific staining and mounted in Fluoromount-G (Thermo Fisher Scientific). The cell morphology, alkaline phosphatase and calcium deposition (alizarin red S) were observed using a light microscope (Axio Vert.A1 inverted microscope, ZEISS, Germany) and images acquired using a camera Axiocam 503 color (Zeiss, Germany). The analysis was carried by using ImageJ Software (National Institute of Mental Health, Bethesda, Maryland, USA).

2.5. Alkaline phosphatase activity

HOEL and MC3T3-E1 (4×10^4 cells) were plated in 24-well plates in MEM with 10% FBS. After 24 h, the adherent cells were cultured in osteogenic medium. After 7, 14 and 28 days, the total cellular protein extract was obtained by lysis buffer containing 10 mmol L^{-1} Tris pH 7.5, 0.5 mmol L^{-1} $MgCl_2$ and 0.1% Triton X-100. The ALP activity was measured by enzymatic assay using *p*-nitrophenyl phosphate (*p*NPP) as a substrate. For the ALP activity assay, a solution containing 25 mmol L^{-1} glycine buffer (pH 9.4), 2 mmol L^{-1} $MgCl_2$ and 1 mmol L^{-1} *p*NPP were added to 96-well plates. After incubation for 30 min in a water bath, each sample was added in duplicate. The plate was kept at 37 °C for a time required for a reaction to occur, and then stopped with 1 mol L^{-1}NaOH. The final product (*p*-nitrophenol) was quantified at 405 nm and the results were expressed as unit of enzyme activity/mg of protein where one unit was defined as the amount of enzyme that converted 1 µ mol L^{-1} of substrate to product per minute. Protein concentrations were determined by the Bradford method.

2.6. DNA methyltransferases inhibition

MC3T3-E1 (25×10^4 cells) were seeded into 6-well plates in Alpha-MEM medium containing antibiotics (100 U/mL penicillin, 100 mg/mL streptomycin), ribonucleosides, and deoxyribonucleosides, supplemented with 10% Fetal Bovine Serum (Nutricell, Campinas, SP, Brazil). After 24 h of incubation at 37 °C in a humidified atmosphere containing 5% CO_2, the cells were treated with 5 µmol L^{-1} of DMNTs inhibitor (SGI-1027 - SML1358, Sigma) and osteogenic differentiation medium (basal culture medium Alpha-MEM supplemented with ascorbic acid at 50 µg/mL, β-glycerolphosphate 10 mmol L^{-1}, dexamethasone 10 nmol L^{-1}, 10% FBS, and penicillin/streptomycin 1%) for 3, 7, 14 and 28 days. The control group was maintained in basal medium alpha-MEM supplemented with 10% FBS and antibiotics.

2.7. RNA isolation, cDNA synthesis and qRT-PCR

Total RNA was extracted from cells with Ambion TRIzol Reagent (Life Sciences - Fisher Scientific Inc., Waltham, MA, USA). The concentration of RNA was measured using the Nanodrop ND-1000 (Wilmington, USA) and treated with DNase I (Invitrogen, Carlsbad, CA, USA). cDNA synthesis was carried out in a total of 20 µL with High Capacity cDNA Reverse Transcription Kit (Applied Biosystems, Foster City, CA) according to the manufacturer's instructions. Quantitative PCR was performed with SYBR Green (Applied Biosystems®, USA) in an IQ5 PCR machine (Bio-Rad) to assess changes in mRNA expression of genes related to osteoblastic differentiation, HOXA gene family cluster and epigenetic machinery control (Table S1) The amount of mRNA present was corrected using the combination of these three genes (*RP2*, *β-ACTIN* and *GAPDH*) (Table S1) using the ΔΔCT method. As threshold value for analyzing the qPCR data 40,000 was chosen. At this threshold value the ΔRn *vs* cycle graphic showed a straight increasing line in the logarithmic view and an exponential increasing line in the absolute view.

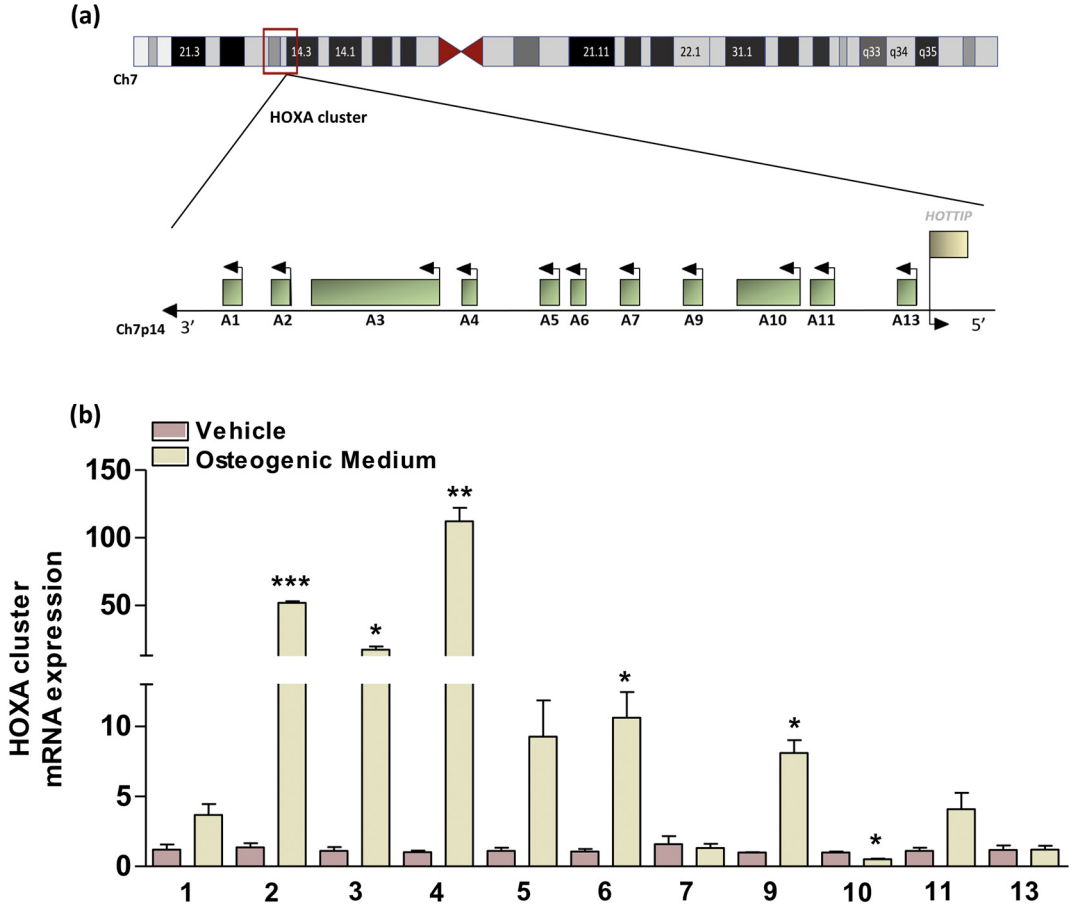

Fig. 2. HOXA gene cluster family expression osteoblast differentiation. (a) Chromosomal structure and organization of the HOXA cluster. (b) HOXA mRNA levels were analyzed by qPCR after 28 days of classical osteogenic differentiation. The relative gene expression levels were determined using the cycle threshold (Ct) method and is depicted in a graphical format with normalized values as a function of the control-assigned value of 1. The results represent mean ± standard deviation of three independent experiments. *p < 0.05, **p < 0.001 and ***p < 0.0001 compared with control.

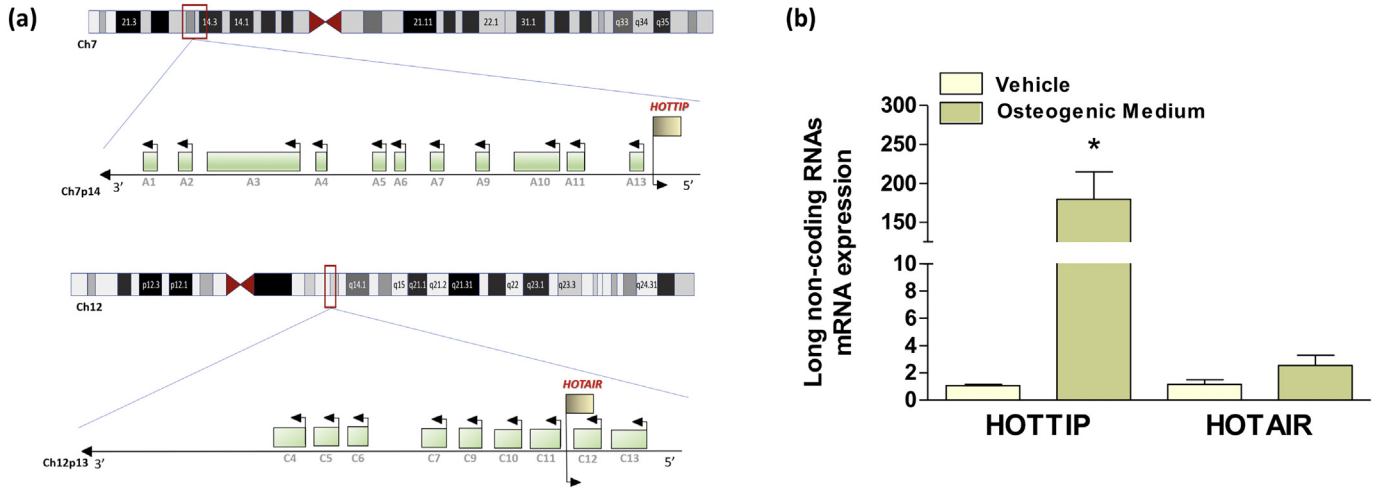

Fig. 3. Effect of osteoblast differentiation on expression of the long chain non-coding RNA (lcnRNA) HOTTIP and HOTAIR. (a) Chromosomal structure and lncRNAs organization of the HOXC cluster, for HOTTIP location, see Fig. 2A. (b) HOTTIP and HOTAIR mRNA levels were analyzed by qPCR after 28 days of osteogenic differentiation. The relative gene expression levels were determined using the cycle threshold (Ct) method and are shown in a graphical format with normalized values as a function of a control-assigned value of 1. The results represent the mean ± standard deviation of three independent experiments. *p < 0.05.

2.8. Epigenetic studies - DNA extraction and treatment

After osteoblastic differentiation, the cells were washed once with PBS, and once in Nuclei Lysis Solution, after which genomic DNA (gDNA) was purified by extraction with phenol/chloroform/isoamyl alcohol. The gDNA concentration was measured using the Nanodrop ND-1000 (Wilmington, USA) and stored at −20 °C. Thereafter, to distinguish amongst DNA methylation and hydroxymethylation the genomic DNA was treated with T4-β-glucosyltransferase (T4-BGT) that adds a glucose moiety only to 5-hydroxymethylcytosine (5-hmC)

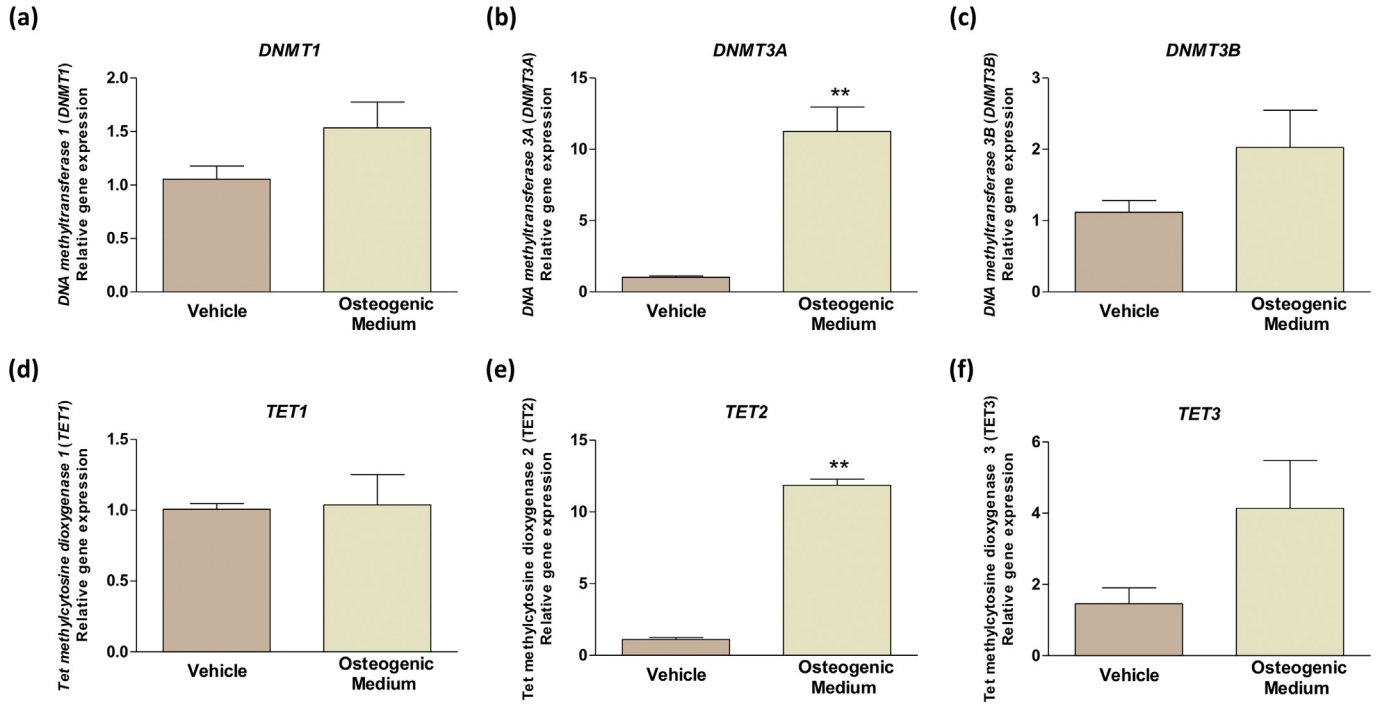

Fig. 4. Effect of osteoblast differentiation on the expression of DNA methylation modifying enzymes. *DNA methyltransferases*, *DNMT1* (a), *DNMT3A* (b) and *DNMT3B* (c) and Teti methylcytosine dioxygenases, *TET1* (d), *TET2* (e) and *TET3* (f) mRNA levels were analyzed by qPCR after 28 days of o*steogenic differentiation*. The relative gene expression levels were determined using the cycle threshold (Ct) method and shown in a graphical format with normalized values as a function of the control-assigned value of 1. The results represent as mean ± standard deviation of three independent experiments. *$p < 0.05$, **$p < 0.001$ and ***$p < 0.0001$.

residues in double-stranded DNA, converting them to beta-glucosyl-5-hydroxymethylcytosine and blocking the *Msp*I activity that can recognize and cleave all CCGG sequences except for glycosylated 5-hmc. For this, gDNA was divided into three tubes containing 400 ng gDNA each, and treated with 1× NE buffer, 40 mmol L^{-1} UDP glucose and T4-BGT (1 unit) to a final volume of 20 µL and incubated at 37 °C for 1 h, followed by 10 min at 65 °C for enzyme inactivation. Afterward, the samples were digested with *Msp*I or *Hpa*II restriction enzymes (New England Biolabs, Beverly, MA, USA) or H_2O (control), to a final volume of 25 µL at 37 °C for 1 h. The tubes containing the *Hpa*II restriction enzyme were submitted to an additional incubation for 10 min. at 65 °C for enzyme inactivation.

2.9. Bisulfite treatment and DNA methylation measurement

To determine DNA methylation profiles, samples underwent bisulfite conversion performed using 500 ng genomic DNA per sample and using the EZ DNA Methylation Kit (Shallow; Zymo Research). Bisulfite converted samples were then hybridized to the Illumina 850 k DNA methylation array (Infinium MethylationEPIC Beadchip; Illumina) according to the manufacturer's instructions. The methylation data of the HOXA Cluster were extracted and analyzed by bioinformatics.

2.10. Gene promoter methylation analysis

For analysis of gene promoter 5-methylcytosine (5-meC) and 5-hydrymethylcytosine (5-hmeC) content, the qPCR was performed in a reaction with 25 µL, containing PowerUp™ SYBR™ Green Master Mix 2× (12.5 µL) (Applied Biosystems, Foster City, CA, USA), 0.5 µmol L^{-1} of each primer, 1 µL of treated gDNA and nuclease free H_2O. All the primers were designed on regulatory regions such as DNaseI hypersensitivity clusters sites, layered by histone modifications marks, CpG regions, and transcription factors binding sites, with Primer3 Input (version 0.4.0) software and analyzed for secondary structures and annealing temperatures by the Beacon Designer (http://www.premierbiosoft.com/). Sequences and chromosome location were confirmed by *in-silico* PCR (https://genome.ucsc.edu/). The characteristics of primers and regions of genes analyzed and PCR conditions are illustrated in Table S2.

2.11. Western blot

The proteins were extracted in 500 µL Laemmli Buffer [SDS 4%, glycerol 20%, Tris-Cl (pH 6.8) 120 mmol L^{-1}, bromophenol blue 0.02% (w/v) and DTT 0.1 mol L^{-1}]. In short, 5 mL protein (50 mg) was resolved by SDS-PAGE and blotted onto Immobilon FL PVDF membranes (Millipore, Bedford, MA, USA). Membranes were blocked in Tris-buffered saline (TBS) with 0.05% Tween 20, albumin 2,5% (TBSTA) and incubated overnight at 4 °C with appropriate primary antibody (Table S3), followed by the appropriate horseradish peroxidase (HRP)-linked secondary antibodies in TBSTA for 1 h an ambient temperature. The immunoreactive bands were detected with enhanced chemiluminescence kit.

2.12. Data analyses

The intensities of methylated and unmethylated signals were normalized using the Illumina GenomeStudio program and graphical representations were performed using R package circlize [35] and GraphPad Prism 5 (GraphPad Software Inc., San Diego, CA, EUA).

2.13. Statistical analyses

All experiments were performed at least three times. Results were expressed as mean ± standard deviation. Statistical analysis was performed by the Student's t using GraphPad Prism 5 (GraphPad Software Inc., San Diego, CA, EUA). Differences were considered significant at $p < 0.05$, representing two-sided test of statistical significance.

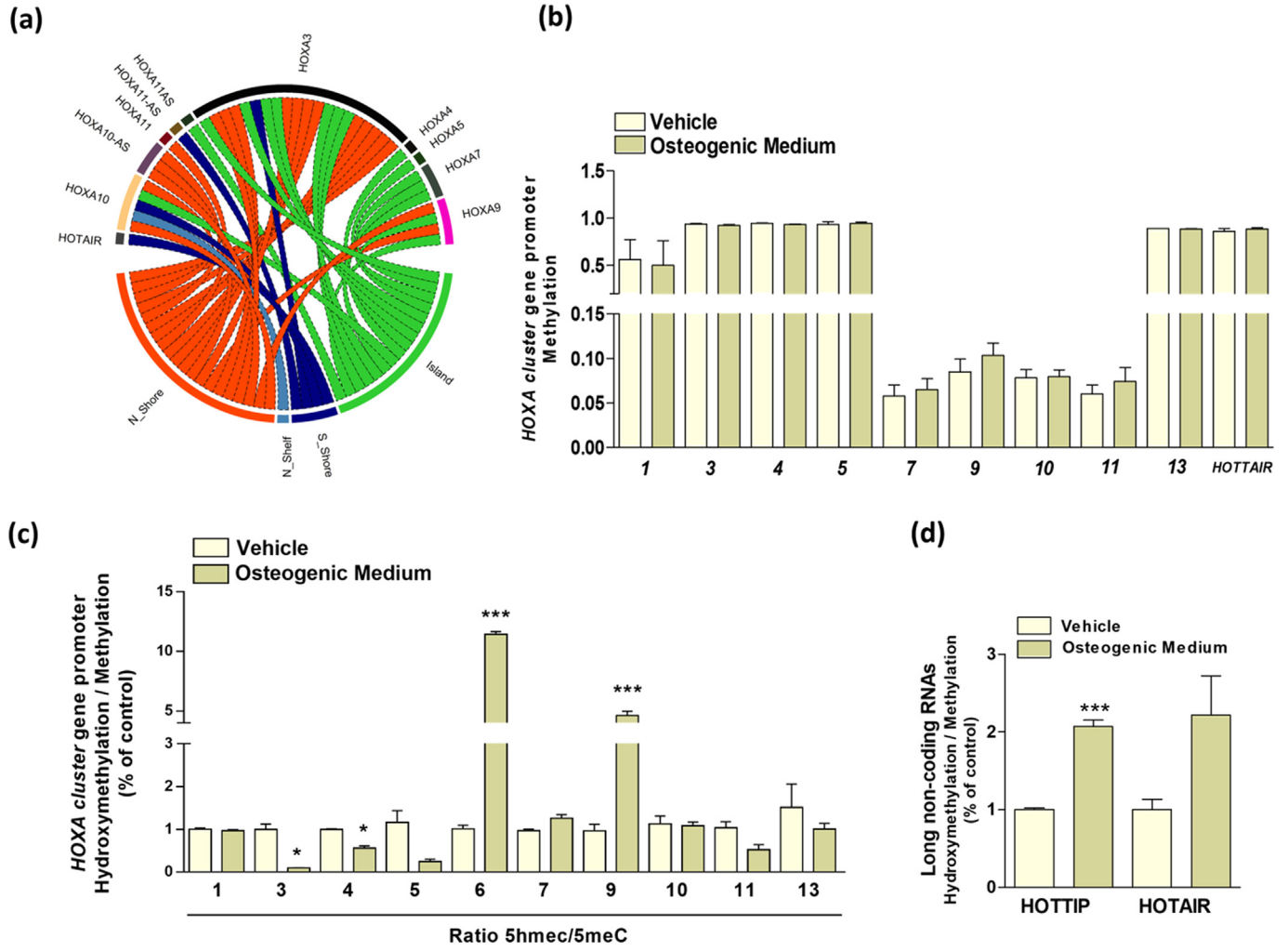

Fig. 5. Epigenetic landscape of HOXA and lncRNA genes during osteoblast differentiation. Gene promoter hydroxymethylation/methylation patterns in HOEL cells were investigated by DNA glucosylation by T4-BGT, followed by *Msp*I and *Hpa*II digestion and qPCR of promoter sequences. The DNA methylation status of the *HOXA* family of genes based on the qPCR data obtained after 28 days of differentiation is shown in a graphical format with normalized values as a function of the control-assigned value of 1 (c), whereas a schematic overview of CpG island organization of the *HOXA* cluster is provided as well (a), which also was represented in the graph (b). Hydroxymethylation/methylation patterns for HOTTIP and HOTAIR in osteoblast differentiation (d). The relative levels were determined using the cycle threshold (Ct) method and the methylation results are presented as HpaII levels - MspI levels/control levels and the hydroxymethylation results are presented as MspI levels-control levels. Results were represented as mean ± standard deviation of three independent experiments. *p < 0.05, **p < 0.001 and ***p < 0.0001.

3. Results

3.1. Description and validation of the osteoblast differentiation strategy

The paucity of data on the regulation of the HOXA cluster during osteoblast differentiation prompted us to investigate this aspect of osteogenesis. Such studies, however, critically depend on the appropriateness of experimental model employed. Various *in vitro* models for bone formation by osteoblasts are being used, including primary rat, ovine, mouse, rabbit, and bovine osteoblast cells; as well as MG-63, MC3T3-E1, and SaOs-2 cell lines. However, these models are either non-human or involve immortalized cells. Thus, we resorted to using primary normal human osteoblast (HOEL) cells, isolated from superfluous bone following surgery. Routinely, when cultured in DMEM for 28 days, these cells have the morphological aspect of relatively undifferentiated precursors with a round shape, an irregularly-formed nucleus with visible nucleoli and dispersed chromatin and a cytoplasm containing well-developed rough endoplasmic reticulum, large Golgi complex, electron dense mitochondria, vesicles and vacuoles containing fibrillar structures as well as secretory granules. In apparent agreement with their status as undifferentiated precursors, expression of *RUNX2*, *OSTERIX*, *ALP*, *OCN* and *COL1A1* mRNA was low (Fig. 1a–c, f, g), whereas expression of *OTN* (Fig. 1e) and *BSP* (not shown) was high. In contrast, when cells were cultured in the presence of 50 µg/mL ascorbic acid, 10 m mol L^{-1} of β-glycerolphosphate and 10 n mol L^{-1} of dexamethasone, they acquired a highly differentiated morphological aspect (Fig. 1h) and accordingly expression of *RUNX2*, *OSTERIX*, *ALP*, *COL1A1*, *OCN* and mRNA expression levels strongly increased (Fig. 1a–c, g, h) whereas expression of *OTN* was decreased (Fig. 1e). In addition, OPN was unchanged in our model (Fig. 1d). OPN and OCN are generally used as early and late hallmarks of osteogenic differentiation respectively, and thus these data suggest that our model represents late rather than early stages of osteogenesis [36]. In apparent agreement, ALP enzymatic activity (Fig. 1i) end alizarin red levels (Fig. 1j) increased in these cultures in line with the postulated late osteogenic events. Finally we compared ALP and Ca^{2+} disposition of HOEL to MC3T3-E1 cells (the latter being an established model system for later late osteogenesis; Fig. 1k, l) and the result again support the notion that HOEL cells can be used for studying osteogenic differentiation. We thus concluded that our experimental set up allows us to assess gene expression in primary human cells in the context of osteoblast differentiation towards an osteogenic phenotype and we decided to

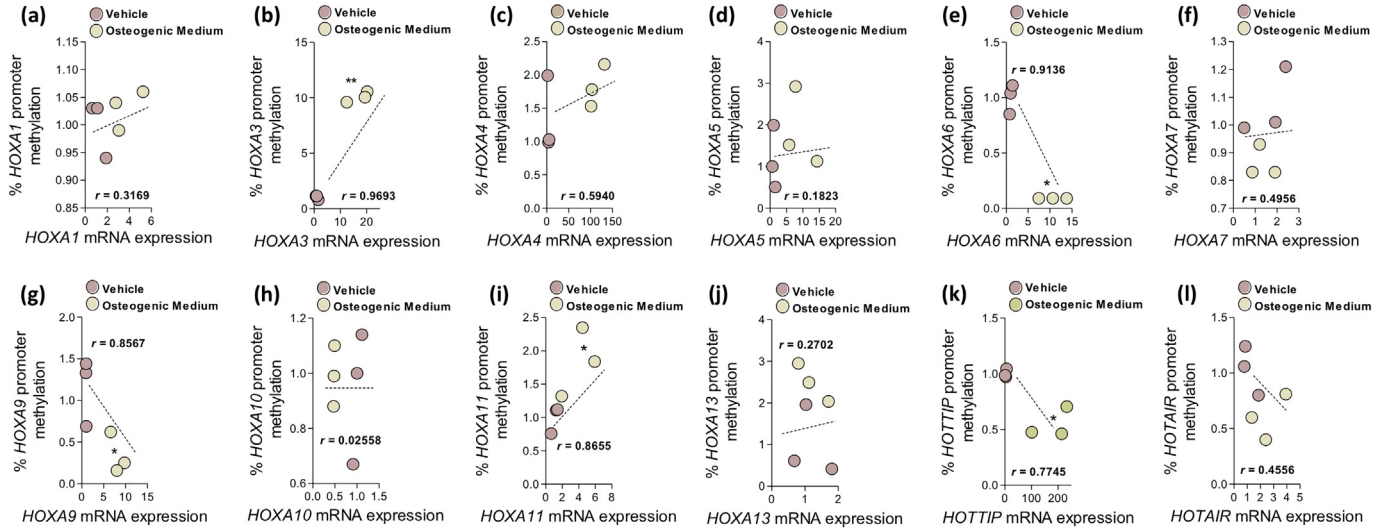

Fig. 6. Relation between promotor methylation status and expression of *HOXA* cluster genes. *HOXA1* (a), *HOXA3* (b), *HOXA4* (c), HOXA5 (d), *HOXA6* (e), *HOXA7* (f), *HOXA9* (g), *HOXA10* (h), *HOXA11* (i), *HOXA13* (j), *HOTTIP* (k) and *HOTAIR* (l) gene promoter methylation/hydroxymethylation pattern in HOEL cells was determined through DNA glucosylation T4-BGT, followed by MspI and HpaII digestion and qPCR of promoter sequences. The relation gene expression and DNA methylation status of the *HOXA* family genes following 28 days of osteoblast differentiation is shown in a graphical format with normalized values as a function of the control-assigned value of 1. The relative levels were determined using the cycle threshold (Ct) method and the methylation results are presented as HpaII levels - MspI levels/control levels and the hydroxymethylation results are presented as MspI levels-control levels. Results were represented as mean ± standard deviation of three independent experiments. *$p < 0.05$, **$p < 0.001$ and ***$p < 0.0001$.

interrogate this set up for effects on the transcriptional activity in the *HOXA* cluster.

Members of the HOXA gene cluster family are differentially expressed during osteoblast differentiation.

To gain a better understanding of the molecular mechanisms driving the osteogenic phenotype of osteoblasts, we evaluated the involvement of all members of the *HOXA* gene family (see Fig. 2a, for an overview of the genomic HOXA cluster structure) in differentiating osteoblast cultures. Importantly, our results showed that osteogenic differentiation is generally associated with a marked upregulation of HOXA gene family expression, suggesting that HOXA coding occurs relatively late during bone formation (Fig. 2b; Fig. S1). In particular we observed a significant increase in expression of *HOXA2* (Fig. 2b; Fig. S1b, ≈ 40-fold change), *HOXA3* (Fig. 2b; Fig. S1c, ≈ 15-fold change), *HOXA4* (Fig. 2b; Fig. S1d, ≈ 100-fold change), *HOXA6* (Fig. 2b; Fig. S1f, ≈ 10-fold change) and *HOXA9* (Fig. 2b; Fig. S1h, ≈ 10-fold change) in comparison in the control cell cultures. Additionally, *HOXA1* (Fig. 2b; Fig. S1a), *HOXA5* and *HOXA11* displayed higher expression during osteogenic differentiation (Fig. 2b; Fig. S1e, j) although these levels did not reach statistical significance, while *HOXA7* and *HOXA13* remained unchanged during differentiation (Fig. 2b; Fig. S1g, l). In contrast, *HOXA10* was significantly down-regulated in differentiated osteoblasts (Fig. 2b; Fig. S1i). Thus, *HOXA* gene patterns are significantly altered during differentiation suggesting that during osteogenic differentiation *HOXA* coding becomes more anterior.

3.2. Regulation of long non-coding RNAs during osteoblast differentiation

Having established a modulation of HOXA genes during osteogenic differentiation, we next wondered which upstream mechanisms might contribute to this phenomenon. Modulation of HOX genes is, amongst others, mediated by long chain non-coding RNAs (lncRNA), regulatory RNA molecules which can both positively and negatively affect transcription and mRNA levels through a number of different ways, including chromatin modification, direct transcriptional regulation and gene silencing through production of endogenous siRNA. HOTTIP and HOTAIR are two such lcnRNA molecules. While HOTTIP is known to positively affect the *HOXA* genes, in particular the more 5′-HOX genes [37,38] (HOXA9 and HOXA13) [39,40], HOTAIR is thought to regulate the HOXD cluster of genes [41]. We evaluated the presence of these lncRNAs in developing osteoblasts (Fig. 3a, b) and observed that expression of HOTTIP was significantly increased, while HOTAIR levels were not significantly changed (Fig. 3b). Thus, these results show that lncRNA expression is subject to regulation during osteoblast differentiation, at least with respect to *HOTTIP*. Nevertheless, lncRNA expression is apparently uncoupled from expression of the coding RNAs in the HOXA cluster, as HOTTIP is canonically associated with upregulation of 5′ *HOXA* members, which is not seen in our data.

3.3. Methylation modifying enzymes are differentially expressed in osteoblasts

Epigenetic changes culminating on methylation profiles are implicated in many biological processes, being decisive for different phenotypes through modulation of gene activations. Based on their importance, we evaluated whether genes encoding DNA methylation modifying enzymes were alternatively expressed in differentiated osteoblasts. Our results showed that only methyltransferase *DNMT3A* showed significant upregulation (Fig. 4b, $p < 0.001$), while *DNMT1* (Fig. 4a) and *DNMT3B* (Fig. 4c) show modest increases in expression. In addition, of the Teti methylcytosine dioxygenases (*TETs*) tested (Fig. 4d–f), only *TET2* demonstrated significant induction of expression upon differentiation as compared with the control cell cultures (Fig. 4e, $p < 0.001$). We thus concluded that although osteoblast differentiation is not subject to gross modifications in methyltransferase expression, specific effects are observed and that the possibility of specific methylation changes in the promoter of *HOXA* cluster genes should be investigated.

3.4. Epigenetic machinery modulates HOXA genes during osteoblast differentiation

In light of the specific transcript profiles of the DNA methylation enzymes and especially the high expression of *DNMT3A* and *TET2* observed during osteoblast differentiation, we decided to evaluate whether *HOXA* and *lncRNAs* genes were epigenetically modified during

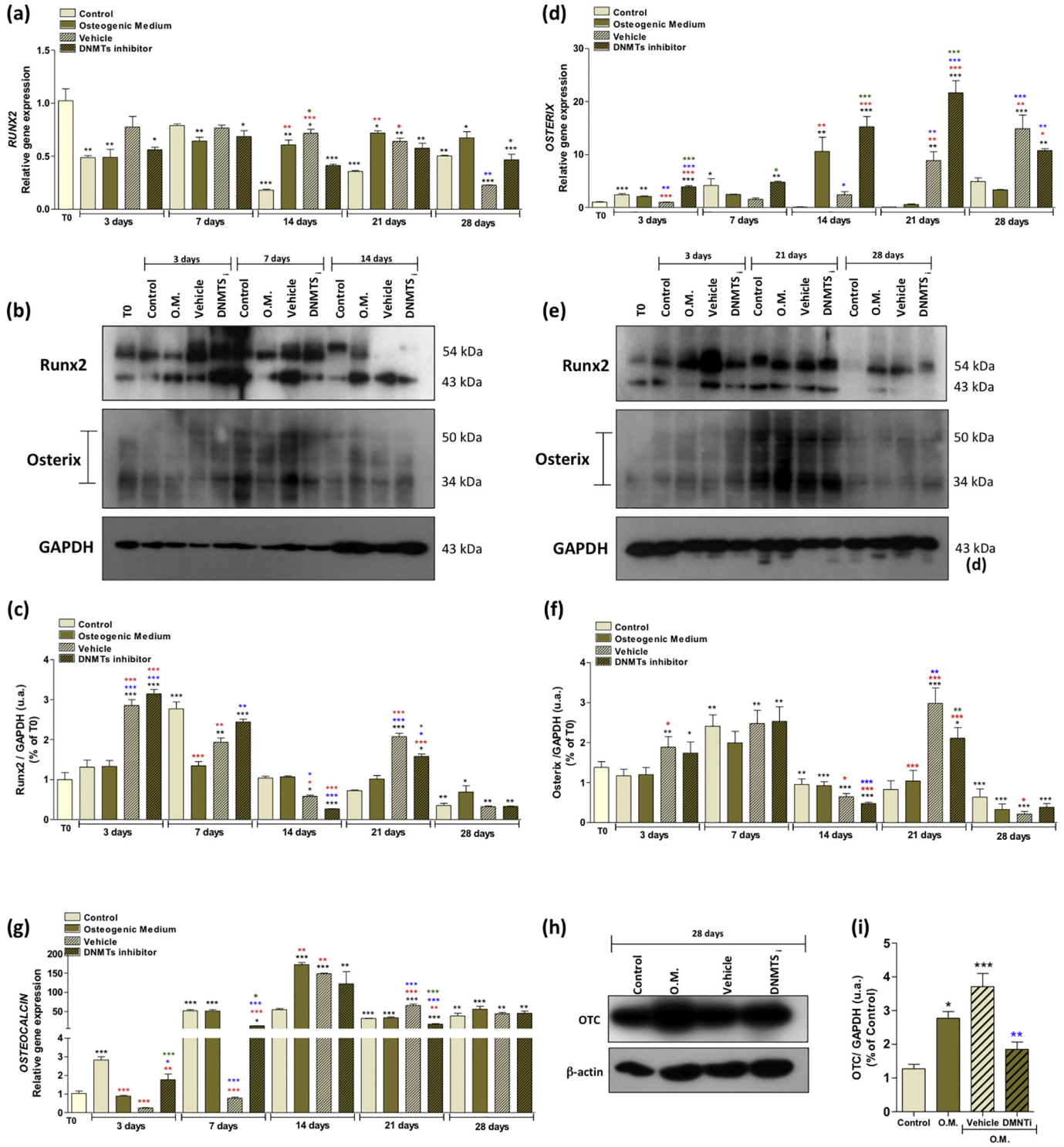

Fig. 7. DNMTs modulate osteoblast gene marker levels. Runt-related transcription factor 2 (*RUNX2*) (a), transcription factor Sp7 (OSTERIX – *OTX*) (d) and *Osteocalcin* (*OTC*) (g) mRNA levels were analyzed by qPCR after 3, 7, 14, 21 and 28 days following o*steogenic differentiation*. (b, e) Representative immunoblots for *RUNX2 (b), OTX* (c) and *OTC* (h). ImageJ Software densitometric analysis of immunoblots (c, f, i), normalized to the protein ratio of controls (1) with GAPDH or β-actin as loading controls. The relative gene expression levels were determined using the cycle threshold (Ct) method and shown in a graphical format with normalized values as a function of the control-assigned value of 1. The results are represented as mean ± standard deviation of three independent experiments. *p < 0.05, **p < 0.001, ***p < 0.0001 when compared with T0 group; *p < 0.05, **p < 0.001, ***p < 0.0001 when compared with Control 3 days; *p < 0.05, **p < 0.001, ***p < 0.0001 when compared with O.M. and *p < 0.05, **p < 0.001, ***p < 0.0001 when compared with Vehicle.

osteoblast differentiation. To this end the Illumina 850 k DNA global methylation array was used to contrast methylation in undifferentiated and differentiated HOEL cells. This platform contains 41 probes measuring methylation in the *HOXA* cluster covering seven different expressed sequences. Of these, twenty probes covered different regions of the *HOXA3* gene of, one probe targeted *HOXA4*, one probe measured *HOXA7*, four probes mapped to *HOXA4*, eight probes were complementary with *HOXA10*, three probes were directed at *HOXA11* and

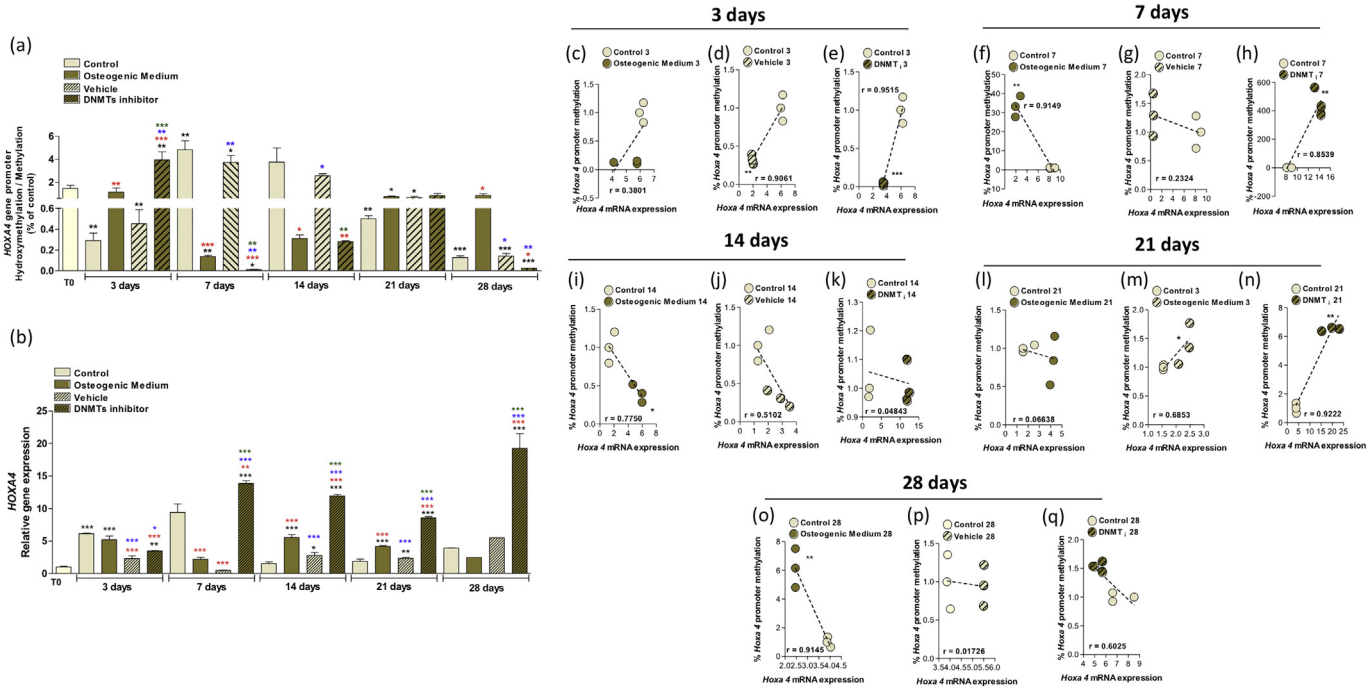

Fig. 8. Effects of DNMT inhibition on HOXA4 during osteoblast differentiation. (a) HOXA4 gene promoter methylation ratio and (b) HOXA4 mRNA levels were investigated in MC3TE after 3, 7, 14, 21 and 28 days of classical osteogenic differentiation by DNA glucosylation by T4-BGT, followed by MspI and HpaII digestion and qPCR of promoter and mRNA sequences. The DNA methylation status of the and gene expression of HOXA4 are shown in a graphical format with normalized values as a function of the control-assigned value of 1 (b) Correlation analysis between gene promoter DNA methylation/hydroxymethylation pattern and gene expression after 3 (c, d, e), 7 (f, g, h), 14 (I, j, k) 21 (l, m, n) and 28 (o, p, q) days of osteoblast differentiation. The DNA methylation status based on the qPCR data obtained after mineralization-inducing medium treatment is shown in a graphical format with normalized values as a function of the control-assigned value of 1. The relative levels were determined using the cycle threshold (Ct) method and the methylation results are presented as HpaII levels - MspI levels/control levels and the hydroxymethylation results are presented as MspI levels-control levels. Results were represented as mean ± standard deviation of three independent experiments. *p < 0.05, **p < 0.001, ***p < 0.0001 when compared with T0 group; *p < 0.05, **p < 0.001, ***p < 0.0001 when compared with Control 3 days; *p < 0.05, **p < 0.001, ***p < 0.0001 when compared with O.M. and *p < 0.05, **p < 0.001, ***p < 0.0001 when compared with Vehicle. Significant positive correlation between r = 0.683 and 1.

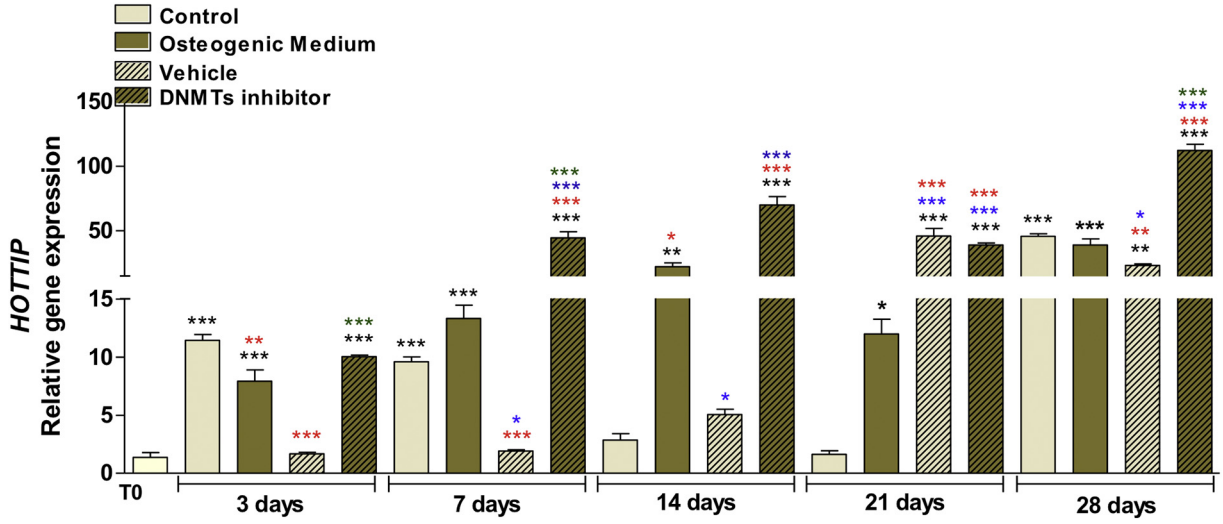

Fig. 9. Effects of DNMT inhibition on HOTTIP expression during osteoblast differentiation. HOTTIP mRNA levels were analyzed by qPCR after 3, 7, 14, 21 and 28 days of osteogenic differentiation in the presence or absence of DNMT inhibitor. The relative gene expression levels were determined using the cycle threshold (Ct) method and shown in a graphical format with normalized values as a function of the control assigned value 1. The results represent the mean ± standard deviation of three independent experiments. *p < 0.05, **p < 0.001, ***p < 0.0001 when compared with T0 group; *p < 0.05, **p < 0.001, ***p < 0.0001 when compared with Control 3 days; *p < 0.05, **p < 0.001, ***p < 0.0001 when compared with O.M. and *p < 0.05, **p < 0.001, ***p < 0.0001 when compared with Vehicle.

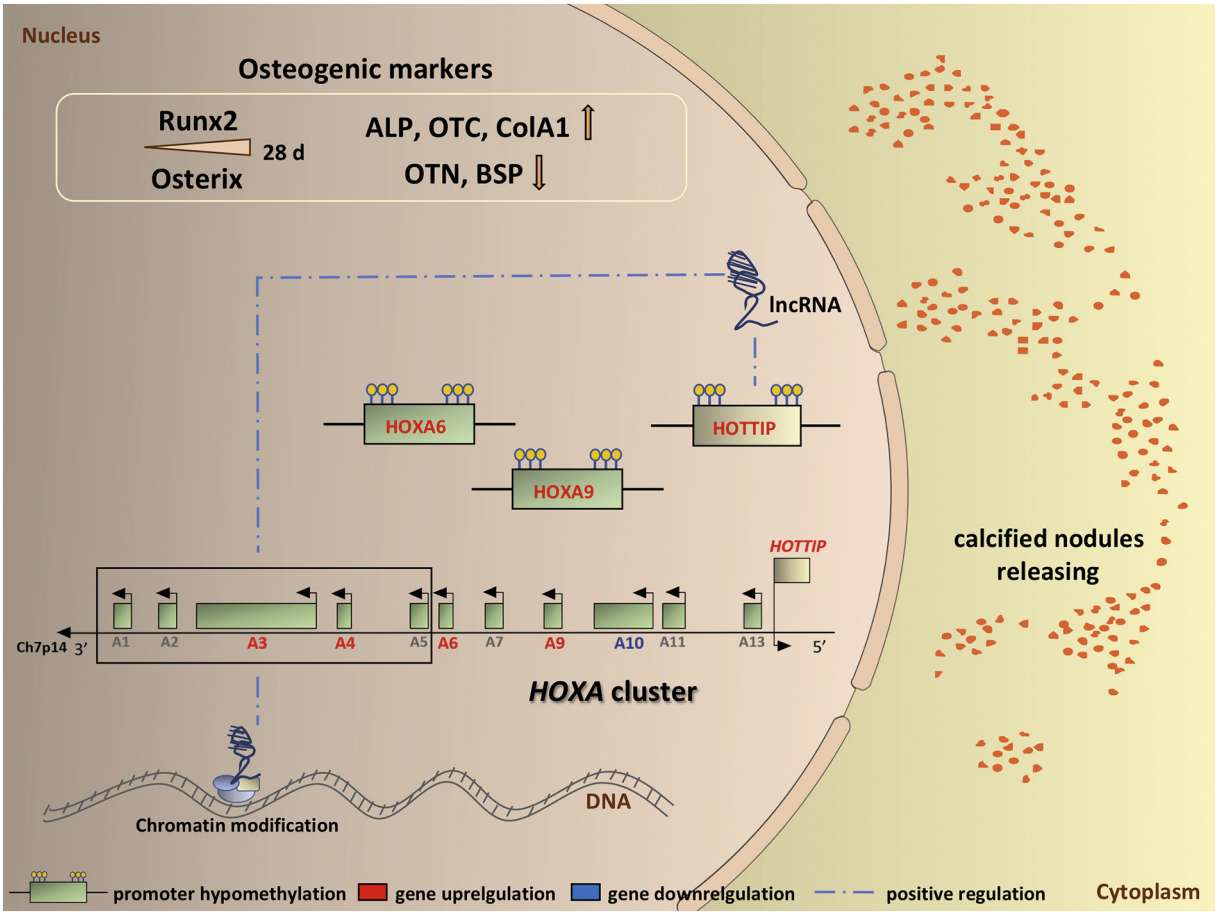

Fig. 10. Schematic depiction of *HOXA* cluster regulation during osteoblast differentiation. Our data suggest HOTTIP as a possible regulatory mediator of five prime *HOXA* genes through multiple mechanisms at least including regulation by differential microRNAs expression and histone methylation. The increase in HOTTIP during osteoblast differentiation is intriguing though and may represent a negative feedback following the down regulation of five prime *HOXA* members. Importantly, for most *HOXA* cluster members, a clear correlation between promoter methylation and expression emerges. Thus promoter methylation constitutes a relevant regulatory effect in expression control of *HOXA* cluster members and altogether drives the osteoblastic phenotype.

one probe was designed to measure the lncRNA – HOTTAIR. In conjunction, these probes allowed investigation of the differential methylation during osteoblastic differentiation of the *HOXA* cluster, which contains various CpG islands, especially at the 5′ end of the cluster (Fig. 5a). An abstraction of the results, collapsed on single orthologue member is provided in Fig. 5b and on first sight seems to indicate that promotor methylation is little changed during osteogenic differentiation and would thus not explain differential expression of *HOXA* cluster members during this process. Taking into account, however, our methodology that involves transformation by bisulfite that does not distinguish the hydroxymethylated cytosine (5-hmC) from methylated cytosine (5mC), we decided to further analyze cytosine methylation status of *HOXA* cluster genes by an enzymatic assay that involves glucosylation of 5hmC by T4 phage β-glucosyltransferase, digestion with *Msp*I or *Hpa*II and qPCR [42]. This assay allows the quantification of methylated cytosine (5mC) and hydroxymethyl cytosine (5hmC), the first product formed during active demethylation. Importantly, calculating the ratio of 5hmeC/5meC represents a measure of the total methylation status of the gene, with higher ratios indicative of demethylation and active transcription [43]. The results are presented in Fig. 5c, d and Fig. S2. No significant changes in methylation patterns of the *HOXA5* (Fig. 5c; Fig. S2d), *HOXA10* (Fig. 5c; Fig. S2h) and *HOTAIR* (Fig. 5d; Fig. S2m) genes were observed. However, all the other genes presented significant changes in methylation status in differentiated osteoblasts compared to control culture cells (Fig. 5c; Fig. S2a–m). As shown in the Fig. 5c, an increased demethylation was observed in particular for the midcluster HOXA genes, whereas the 5-HOXA genes showed a decreased methylation pattern. Specifically, 5hmeC/5meC ratios were significantly upregulated for the HOXA6 and HOXA9 during osteogenic differentiation, providing a rational explanation for the increase in expression of these *HOXA* cluster members during osteogenic differentiation. In contrast significantly lower 5hmeC/5meC ratios were observed for HOXA3 and HOXA4, showing uncoupling of *HOXA* cluster methylation and gene expression for these cluster members. For the enzymes HOTTIP and HOTAIR (Fig. 5d), methylation patterns were consistent with their expression profiles, *i.e.*, HOTTIP showed significantly increased demethylation, consistent with increased expression profile, while methylation status was not significantly altered for HOTAIR. Thus, promoter methylation emerges as a critical mediator for *HOXA* cluster regulation in osteogenesis.

This notion was supported in a further analysis of the relationship between the expression of the HOX genes and their promoter methylation status, where we tested the correlation between the epigenetic-based changes with the effective expression of corresponding genes (Fig. 6). Correlations with a Pearson's product moment above r = 0.6 were observed for the *HOXA* genes *3*, *6*, *9*, *11* and *HOTTIP*. For *HOXA6* (r = 0.9693, Fig. 6e), *HOXA9* (r = 0.8567, Fig. 6g) and *HOTTIP* (r = 0.7745; Fig. 6k) mRNA levels are inversely proportional to the methylation status of the promoter region, suggesting that methylation is a major driving force driving expression during osteoblast differentiation for these genes. The inverse correlations observed for *HOXA3* and *HOXA11* reveal the activity of as yet uncharacterized mechanisms

driving gene expression and most likely reflect methylation as a negative feedback on these mechanisms. In conjunction, however, these data show that methylation is important for controlling *HOXA* cluster activity and adapts to other mechanisms driving expression.

3.5. DNMT drives HOXA gene activities during osteogenic phenotype acquisition

DNMTs are attractive candidates for regulating gene expression during osteogenic differentiation. Thus, we decided to block the activity of DNMTs during osteoblast differentiation in order to establish their involvement and necessity in this process. To assess their potential involvement directly, we tested the effect of 5 μ mol L^{-1} of the pharmacological DNMT inhibitor SGI-1027 on gene expression and our data shows significant effects of this treatment on both Runx2 and Osterix genes, Runx2 expression being downregulated in SGI-1027-treated cells relative to vehicle controls during osteogenc differentiation (Fig. 7a). In contrast, inhibition of the DNMTs upregulated Osterix expression (Fig. 7b), strongly suggesting epigenetic control of this gene during osteoblast differentiation. These changes in mRNA levels following DNMT inhibition, however, were only partially reflected in altered protein levels of Runx2 and Osterix (Fig. 7b–f), showing that inhibition of DNMTs effects gene expression at multiple levels. A late biomarker for osteoblast differentiation, Osteocalcin (OTC), was also evaluated for the effect of DNMT inhibition and the data shows that in the absence of DNMT activity expression of this late marker is substantially temporally enhanced at the mRNA level (Fig. 7g). An overview of the effects of DNMT inhibition on methylation-modulating genes themselves during osteoblast differentiation is provided in Fig. S3 and shows that this group of enzymes is indeed an important regulator of gene expression during osteoblast differentiation.

Thus, encouraged we further evaluated the effect of inhibiting DNMT enzymatic activity on the transcription of *HOXA* genes, focusing on *HOXA4* (Fig. 8) and *HOXA9* (Fig. 9). Fig. 8 shows a positive correlation between *HOXA4* promotor methylation and expression, while the inhibition of DNMTs provoked down-regulation of *HOXA4* promotor methylation (Fig. 8a), showing the importance of DNMTs for maintaining *HOXA4* promotor methylation. DNMT inhibition provoked increased *HOXA4* transcription (Fig. 8b) thus DNMTs likely act as a feedback mechanism downstream of *HOXA4* action limiting over-activation of its activity. This notion was supported in a further analysis of the relationship between the expression of the *HOXA4* and 9 genes and their promoter methylation status, where we tested the correlation between the epigenetic-based changes with the effective expression of corresponding genes (Fig. 8c–q; Fig. S4c–q; respectively), where correlations with a Pearson's product moment above r = 0.6 were observed for the *HOXA* genes. In addition, we observed that DNMTs modulate HOTTIP gene activity by epigenetic control of its promoter region (Fig. 9).

4. Discussion

Although it is evident that the skeletal phenotype depends to a large extent on HOX coding, there is remarkably little information as to the molecular mechanisms that control expression of individual paralogue members. This situation also holds true for the *HOXA* cluster, the subject of the current study. Extrapolating from other systems, it has been proposed that the HOX gene cluster lncRNAs HOTAIR and especially HOTTIP are important regulatory factors in this respect, with HOTTIP an important positive regulatory mediator of 5′-*HOXA* genes through a plethora of mechanisms including regulation of microRNAs and histone methylation [44]. The current study found, however, little evidence for this as HOTTIP increased during osteoblastic differentiation, whereas expression of 5′-*HOXA* cluster members in general showed a decreasing trend. Expression levels of HOTAIR were little correlated to osteoblast differentiation and expression of specific paralogue members (not shown), and thus the lncRNAs do not seem very important in this respect. The increase in HOTTIP during osteoblast differentiation *per se* is intriguing though and may even represent a negative feedback effect on the down regulation of 5′-*HOXA* members (Fig. 10). Importantly, for most *HOXA* cluster members a clear correlation between promoter methylation and expression emerges. Thus we are forced to conclude that promoter methylation constitutes a relevant regulatory effect in expression control of *HOXA* cluster members. However, it is important to note that other regulatory mechanisms, including the expression of miRNAs, have also been shown to modulate the expression of HOXA genes during osteoblast generation by regulating histone acetylation [45], adding a further layer of complexity to this system.

Our data show that concomitant with osteoblastic differentiation, *HOXA* cluster member expression is elaborately regulated, in line with the conventional view that this cluster is important for determining cell fate in this process. *HOXA* cluster involvement in osteogenesis is clearly complex and involves differential regulation of these genes in different cell compartments [26]. In the current study, rostral-caudal positional clues were absent due to the *in vitro* nature of our model system, which may have influenced results, but our results clearly support the notion that *HOX* coding is relevant during osteogenesis. In this sense the comparison with leukemic and myelodysplastic syndromes may be relevant. Of note, in these diseases aberrant cellular proliferation is driven by increased expression of *HOXA9* and we observe that osteoblast differentiation (which is associated by cessation of the cell cycle) is associated by the involvement of *HOXA9* expression. It should thus prove interesting to investigate whether *HOXA9* drives similar transcriptional responses in this context. The fact that both in hematological malignancies and osteoblast differentiation altered *HOXA9* promoter methylation drives alternative expression would support the idea that mechanistic principles might be comparable and we call for further research in this aspect of *HOXA9* biology.

Although the strong correlations between *HOXA* cluster member promoter methylation and *HOXA* cluster member expression support a mechanistic connection between these two molecular biological processes, exact interpretation of our data is hampered by the observation that the correlations observed are, although statistically significant, both negative and positive. We interpret our findings as showing that for some *HOXA* cluster members methylation is a dominant factor negatively driving expression levels, while for various other *HOXA* cluster members it reflects the activity of biological negative feedback, not important for influencing expression in the context of the experimental system chosen. In this context it is important to note that although the analyses performed strongly support that our system is a *bona fide* representation of osteoblast differentiation it remains artificial and the concentration of the differentiating agents is in excess as to what might be expected *in vivo*. It is thus possible that in a physiological situation promoter methylation becomes a dominant mechanism for regulating expression levels for all *HOXA* cluster members and that the positive correlations observed for some paralogue members represent feedback response to the artificial conditions employed. Further research is needed to address this issue, but in general our data reveal an important role for the epigenetic landscape in driving *HOXA* cluster member expression during osteoblast differentiation.

It is becoming increasingly clear that physiological regenerative processes in adults depend to a large extent on the same signaling pathways as those activated during embryogenesis [46]. Several studies have now shown that adult bone maintains the expression of the *HOX* genes that exert an important function during embryological steps and bone healing [47,48], and that these genes are essential for modulating osteogenic gene markers such as Alkaline phosphatase, bone sialoprotein, osteocalcin and Runx2. A sequential requirement of these genes during the well-defined steps of osteoblastic differentiation has been postulated [26,49,50]. Interestingly, positional information derived from HOX gene expression during embryological stages may also

determine bone healing in adult tissue. It has been shown that progenitor cells from different skeletal locations demonstrate different HOX gene expression patterns, and that differential modulation of these HOX genes contributes to proper bone regeneration [51]. A better understanding of HOX gene expression patterns and the physiological modulation thereof during osteogenic differentiation may provide additional information into the conserved processes that contribute to healthy regeneration.

Supplementary data to this article can be found online at https://doi.org/10.1016/j.bone.2019.04.026.

Acknowledgements

The authors are grateful to FAPESP (grant nrs 2014/22689-3; 2017/01046-5; 2016/01139-0) and CNPq (PQ2) for the financial support.

References

[1] D.R. Rux, J.Y. Song, K.M. Pineault, G.S. Mandair, I.T. Swinehart, A.J. Schlientz, K.N. Garthus, S.A. Goldstein, K.M. Kozloff, D.M. Wellik, Hox11 function is required for region-specific fracture repair, J. Bone Miner. Res. 32 (2017) 1750–1760, https://doi.org/10.1002/jbmr.3166.

[2] D.R. Rux, D.M. Wellik, Hox genes in the adult skeleton: novel functions beyond embryonic development, Dev. Dyn. 246 (2017) 310–317, https://doi.org/10.1002/dvdy.24482.

[3] N.M. Brooke, J. Garcia-Fernandez, P.W. Holland, The ParaHox gene cluster is an evolutionary sister of the Hox gene cluster, Nature. 392 (1998) 920–922, https://doi.org/10.1038/31933.

[4] A. Amores, A. Force, Y.L. Yan, L. Joly, C. Amemiya, A. Fritz, R.K. Ho, J. Langeland, V. Prince, Y.L. Wang, M. Westerfield, M. Ekker, J.H. Postlethwait, Zebrafish hox clusters and vertebrate genome evolution, Science. 282 (1998) 1711–1714.

[5] C.J. Tabin, R.L. Johnson, Developmental biology: clocks and hox, Nature. 412 (2001) 780–781, https://doi.org/10.1038/35090677.

[6] A. Meyer, Hox gene variation and evolution, Nature. 391 (1998) 225,227–228, https://doi.org/10.1038/34530.

[7] D. Lemons, W. McGinnis, Genomic evolution of Hox gene clusters, Science. 313 (2006) 1918–1922, https://doi.org/10.1126/science.1132040.

[8] G. Andrey, D. Duboule, SnapShot: Hox gene regulation, Cell. 156 (2014) 856–856.e1, https://doi.org/10.1016/j.cell.2014.01.060.

[9] T. Kondo, D. Duboule, Breaking colinearity in the mouse HoxD complex, Cell. 97 (1999) 407–417.

[10] N. Di-Poi, J.I. Montoya-Burgos, H. Miller, O. Pourquie, M.C. Milinkovitch, D. Duboule, Changes in Hox genes' structure and function during the evolution of the squamate body plan, Nature. 464 (2010) 99–103, https://doi.org/10.1038/nature08789.

[11] D. Noordermeer, M. Leleu, E. Splinter, J. Rougemont, W. De Laat, D. Duboule, The dynamic architecture of Hox gene clusters, Science. 334 (2011) 222–225, https://doi.org/10.1126/science.1207194.

[12] S. Xue, S. Tian, K. Fujii, W. Kladwang, R. Das, M. Barna, RNA regulons in Hox 5' UTRs confer ribosome specificity to gene regulation, Nature. 517 (2015) 33–38, https://doi.org/10.1038/nature14010.

[13] K.C. Wang, Y.W. Yang, B. Liu, A. Sanyal, R. Corces-Zimmerman, Y. Chen, B.R. Lajoie, A. Protacio, R.A. Flynn, R.A. Gupta, J. Wysocka, M. Lei, J. Dekker, J.A. Helms, H.Y. Chang, A long noncoding RNA maintains active chromatin to coordinate homeotic gene expression, Nature. 472 (2011) 120–124, https://doi.org/10.1038/nature09819.

[14] R.A. Gupta, N. Shah, K.C. Wang, J. Kim, H.M. Horlings, D.J. Wong, M.-C. Tsai, T. Hung, P. Argani, J.L. Rinn, Y. Wang, P. Brzoska, B. Kong, R. Li, R.B. West, M.J. van de Vijver, S. Sukumar, H.Y. Chang, Long non-coding RNA HOTAIR reprograms chromatin state to promote cancer metastasis, Nature. 464 (2010) 1071–1076, https://doi.org/10.1038/nature08975.

[15] F. Santagati, M. Minoux, S.-Y. Ren, F.M. Rijli, Temporal requirement of Hoxa2 in cranial neural crest skeletal morphogenesis, Development. 132 (2005) 4927–4936, https://doi.org/10.1242/dev.02078.

[16] O. Chisaka, T.S. Musci, M.R. Capecchi, Developmental defects of the ear, cranial nerves and hindbrain resulting from targeted disruption of the mouse homeobox gene Hox-1.6, Nature 355 (1992) 516–520, https://doi.org/10.1038/355516a0.

[17] T. Lufkin, A. Dierich, M. LeMeur, M. Mark, P. Chambon, Disruption of the Hox-1.6 homeobox gene results in defects in a region corresponding to its rostral domain of expression, Cell. 66 (1991) 1105–1119.

[18] M. Gendron-Maguire, M. Mallo, M. Zhang, T. Gridley, Hoxa-2 mutant mice exhibit homeotic transformation of skeletal elements derived from cranial neural crest, Cell. 75 (1993) 1317–1331.

[19] P.P.R. Iyyanar, A.J. Nazarali, Hoxa2 Inhibits Bone Morphogenetic Protein Signaling during Osteogenic Differentiation of the Palatal Mesenchyme, Front. Physiol. 8 (2017) 929, , https://doi.org/10.3389/fphys.2017.00929.

[20] J.L. Chojnowski, H.A. Trau, K. Masuda, N.R. Manley, Temporal and spatial requirements for Hoxa3 in mouse embryonic development, Dev. Biol. 415 (2016) 33–45, https://doi.org/10.1016/j.ydbio.2016.05.010.

[21] P. Hunt, M. Gulisano, M. Cook, M.H. Sham, A. Faiella, D. Wilkinson, E. Boncinelli, R. Krumlauf, A distinct Hox code for the branchial region of the vertebrate head, Nature. 353 (1991) 861–864, https://doi.org/10.1038/353861a0.

[22] O. Chisaka, M.R. Capecchi, Regionally restricted developmental defects resulting from targeted disruption of the mouse homeobox gene hox-1.5, Nature. 350 (1991) 473–479, https://doi.org/10.1038/350473a0.

[23] N. Wery, M.G. Narotsky, N. Pacico, R.J. Kavlock, J.J. Picard, F. Gofflot, Defects in cervical vertebrae in boric acid-exposed rat embryos are associated with anterior shifts of hox gene expression domains, Birth Defects Res. A. Clin. Mol. Teratol. 67 (2003) 59–67, https://doi.org/10.1002/bdra.10031.

[24] R. Balling, G. Mutter, P. Gruss, M. Kessel, Craniofacial abnormalities induced by ectopic expression of the homeobox gene Hox-1.1 in transgenic mice, Cell. 58 (1989) 337–347.

[25] C. Fromental-Ramain, X. Warot, S. Lakkaraju, B. Favier, H. Haack, C. Birling, A. Dierich, P. Doll e, P. Chambon, Specific and redundant functions of the paralogous Hoxa-9 and Hoxd-9 genes in forelimb and axial skeleton patterning, Development. 122 (1996) 461–472.

[26] M.Q. Hassan, R. Tare, S.H. Lee, M. Mandeville, B. Weiner, M. Montecino, A.J. van Wijnen, J.L. Stein, G.S. Stein, J.B. Lian, HOXA10 controls osteoblastogenesis by directly activating bone regulatory and phenotypic genes, Mol. Cell. Biol. 27 (2007) 3337–3352, https://doi.org/10.1128/MCB.01544-06.

[27] D.P. Mortlock, J.W. Innis, Mutation of HOXA13 in hand-foot-genital syndrome, Nat. Genet. 15 (1997) 179–180, https://doi.org/10.1038/ng0297-179.

[28] S.M. Gough, C.I. Slape, P.D. Aplan, NUP98 gene fusions and hematopoietic malignancies: common themes and new biologic insights, Blood. 118 (2011) 6247–6257, https://doi.org/10.1182/blood-2011-07-328880.

[29] A. Rio-Machin, G. Gomez-Lopez, J. Munoz, F. Garcia-Martinez, A. Maiques-Diaz, S. Alvarez, R.N. Salgado, M. Shrestha, R. Torres-Ruiz, C. Haferlach, M.J. Larrayoz, M.J. Calasanz, J. Fitzgibbon, J.C. Cigudosa, The molecular pathogenesis of the NUP98-HOXA9 fusion protein in acute myeloid leukemia, Leukemia. 31 (2017) 2000–2005, https://doi.org/10.1038/leu.2017.194.

[30] N. Cahill, R. Rosenquist, Uncovering the DNA methylome in chronic lymphocytic leukemia, Epigenetics. 8 (2013) 138–148, https://doi.org/10.4161/epi.23439.

[31] G. Strathdee, T.L. Holyoake, A. Sim, A. Parker, D.G. Oscier, J.V. Melo, S. Meyer, T. Eden, A.M. Dickinson, J.C. Mountford, H.G. Jorgensen, R. Soutar, R. Brown, Inactivation of HOXA genes by hypermethylation in myeloid and lymphoid malignancy is frequent and associated with poor prognosis, Clin. Cancer Res. 13 (2007) 5048–5055, https://doi.org/10.1158/1078-0432.CCR-07-0919.

[32] M.M. Pradeepa, F. McKenna, G.C.A. Taylor, H. Bengani, G.R. Grimes, A.J. Wood, S. Bhatia, W.A. Bickmore, Psip1/p52 regulates posterior Hoxa genes through activation of lncRNA Hottip, PLoS Genet. 13 (2017) e1006677, , https://doi.org/10.1371/journal.pgen.1006677.

[33] L. Li, B. Liu, O.L. Wapinski, M.-C. Tsai, K. Qu, J. Zhang, J.C. Carlson, M. Lin, F. Fang, R.A. Gupta, J.A. Helms, H.Y. Chang, Targeted disruption of Hotair leads to homeotic transformation and gene derepression, Cell Rep. 5 (2013) 3–12, https://doi.org/10.1016/j.celrep.2013.09.003.

[34] B. Wei, W. Wei, B. Zhao, X. Guo, S. Liu, Long non-coding RNA HOTAIR inhibits miR-17-5p to regulate osteogenic differentiation and proliferation in non-traumatic osteonecrosis of femoral head, PLoS One. 12 (2017) e0169097, , https://doi.org/10.1371/journal.pone.0169097.

[35] Z. Gu, L. Gu, R. Eils, M. Schlesner, B. Brors, circlize implements and enhances circular visualization in R, Bioinformatics. 30 (2014) 2811–2812.

[36] J.E. Aubin, Regulation of osteoblast formation and function, Rev. Endocr. Metab. Disord. 2 (2001) 81–94.

[37] Y.W. Yang, R.A. Flynn, Y. Chen, K. Qu, B. Wan, K.C. Wang, M. Lei, H.Y. Chang, Essential role of lncRNA binding for WDR5 maintenance of active chromatin and embryonic stem cell pluripotency, Elife. 3 (2014) e02046, , https://doi.org/10.7554/eLife.02046.

[38] L. Quagliata, M.S. Matter, S. Piscuoglio, L. Arabi, C. Ruiz, A. Procino, M. Kovac, F. Moretti, Z. Makowska, T. Boldanova, J.B. Andersen, M. Hammerle, L. Tornillo, M.H. Heim, S. Diederichs, C. Cillo, L.M. Terracciano, Long noncoding RNA HOTTIP/HOXA13 expression is associated with disease progression and predicts outcome in hepatocellular carcinoma patients, Hepatology. 59 (2014) 911–923, https://doi.org/10.1002/hep.26740.

[39] R. Malek, R.P. Gajula, R.D. Williams, B. Nghiem, B.W. Simons, K. Nugent, H. Wang, K. Taparra, G. Lemtiri-Chlieh, A.R. Yoon, L. True, S.S. An, T.L. DeWeese, A.E. Ross, E.M. Schaeffer, K.J. Pienta, P.J. Hurley, C. Morrissey, P.T. Tran, TWIST1-WDR5-Hottip regulates Hoxa9 chromatin to facilitate prostate cancer metastasis, Cancer Res. 77 (2017) 3181–3193, https://doi.org/10.1158/0008-5472.CAN-16-2797.

[40] C. Lin, Y. Wang, Y. Wang, S. Zhang, L. Yu, C. Guo, H. Xu, Transcriptional and posttranscriptional regulation of HOXA13 by lncRNA HOTTIP facilitates tumorigenesis and metastasis in esophageal squamous carcinoma cells, Oncogene. 36 (2017) 5392–5406, https://doi.org/10.1038/onc.2017.133.

[41] D.-C. Wu, S.S.W. Wang, C.-J. Liu, K. Wuputra, K. Kato, Y.-L. Lee, Y.-C. Lin, M.-H. Tsai, C.-C. Ku, W.-H. Lin, S.-W. Wang, S. Kishikawa, M. Noguchi, C.-C. Wu, Y.-T. Chen, C.-Y. Chai, C.-L.S. Lin, K.-K. Kuo, Y.-H. Yang, H. Miyoshi, Y. Nakamura, S. Saito, K. Nagata, C.-S. Lin, K.K. Yokoyama, Reprogramming antagonizes the oncogenicity of HOXA13-long noncoding RNA HOTTIP axis in gastric cancer cells, Stem Cells. 35 (2017) 2115–2128, https://doi.org/10.1002/stem.2674.

[42] K. Tsumagari, C. Baribault, J. Terragni, S. Chandra, C. Renshaw, Z. Sun, L. Song, G.E. Crawford, S. Pradhan, M. Lacey, M. Ehrlich, DNA methylation and differentiation: HOX genes in muscle cells, Epigenetics Chromatin. 6 (2013) 25, https://doi.org/10.1186/1756-8935-6-25.

[43] M. Mellen, P. Ayata, S. Dewell, S. Kriaucionis, N. Heintz, MeCP2 binds to 5hmC enriched within active genes and accessible chromatin in the nervous system, Cell. 151 (2012) 1417–1430, https://doi.org/10.1016/j.cell.2012.11.022.

[44] B. De Kumar, R. Krumlauf, HOXs and lincRNAs: two sides of the same coin, Sci.

Adv. 2 (2016) e1501402, , https://doi.org/10.1126/sciadv.1501402.
[45] T.C. Godfrey, B.J. Wildman, M.M. Beloti, A.G. Kemper, E.P. Ferraz, B. Roy, M. Rehan, L.H. Afreen, E. Kim, C.J. Lengner, Q. Hassan, The microRNA-23a cluster regulates the developmental HoxA cluster function during osteoblast differentiation, J. Biol. Chem. 293 (2018) 17646–17660, https://doi.org/10.1074/jbc.RA118.003052.
[46] M.F. Pittenger, A.M. Mackay, S.C. Beck, R.K. Jaiswal, R. Douglas, J.D. Mosca, M.A. Moorman, D.W. Simonetti, S. Craig, D.R. Marshak, Multilineage potential of adult human mesenchymal stem cells, Science. 284 (1999) 143–147.
[47] S. Liedtke, A. Buchheiser, J. Bosch, F. Bosse, F. Kruse, X. Zhao, S. Santourlidis, G. Kogler, The HOX Code as a “biological fingerprint” to distinguish functionally distinct stem cell populations derived from cord blood, Stem Cell Res. 5 (2010) 40–50, https://doi.org/10.1016/j.scr.2010.03.004.
[48] D.R. Rux, J.Y. Song, I.T. Swinehart, K.M. Pineault, A.J. Schlientz, K.G. Trulik, S.A. Goldstein, K.M. Kozloff, D. Lucas, D.M. Wellik, Regionally restricted Hox function in adult bone marrow multipotent mesenchymal stem/stromal cells, Dev. Cell. 39 (2016) 653–666, https://doi.org/10.1016/j.devcel.2016.11.008.
[49] W.F. Zambuzzi, J.M. Granjeiro, K. Parikh, S. Yuvaraj, M.P. Peppelenbosch, C.V. Ferreira, Modulation of Src activity by low molecular weight protein tyrosine phosphatase during osteoblast differentiation, Cell. Physiol. Biochem. 22 (2008) 497–506, https://doi.org/10.1159/000185506.
[50] H.R. Kang, C.J. da Costa Fernandes, R.A. da Silva, V.R.L. Constantino, I.H.J. Koh, W.F. Zambuzzi, Mg-Al and Zn-Al layered double hydroxides promote dynamic expression of marker genes in osteogenic differentiation by modulating mitogen-activated protein kinases, Adv. Healthc. Mater. 7 (2018), https://doi.org/10.1002/adhm.201700693.
[51] P. Leucht, J.-B. Kim, R. Amasha, A.W. James, S. Girod, J.A. Helms, Embryonic origin and Hox status determine progenitor cell fate during adult bone regeneration, Development. 135 (2008) 2845–2854, https://doi.org/10.1242/dev.023788.